Advances in Science and Technology Research Journal

Advances in Science and Technology Research Journal, 2026, 20(4), 492–504
https://doi.org/10.12913/22998624/214998
ISSN 2299-8624, License CC-BY 4.0

Received: 2025.11.21
Accepted: 2026.02.15
Published: 2026.03.01

Effects of natural waxes on the physicochemical properties of starch packaging fabricated by compression molding

Magdalena Stepczyńska[1*], Aleksandra Śpionek[1]

[1] Department of Materials Engineering, Kazimierz Wielki University, ul. JK Chodkiewicza 30, 85-064 Bydgoszcz, Poland
* Corresponding author's e-mail: m.stepczynska@ukw.edu.pl

ABSTRACT

This study examines the modification of thermoplastic starch (TPS) with natural waxes (beeswax, jojoba, and carnauba) in order to tailor the thermal, mechanical, and surface properties of starch-based biocomposites for sustainable packaging applications. TPS was blended with waxes at concentrations from 1 to 50 wt% and processed by compression molding. Thermogravimetric analysis (TGA), differential scanning calorimetry (DSC), and dynamic mechanical analysis (DMA) were used to characterize thermal stability, melting transitions, and viscoelastic behavior. Surface wettability was assessed via contact-angle measurements, and morphology was examined using scanning electron microscopy (SEM). The results demonstrate that the type and concentration of wax strongly affect TPS structure and performance. TGA revealed that carnauba slightly increases thermal stability, while jojoba reduces the onset of degradation at higher contents. DSC showed systematic changes in melting endotherms associated with the formation or disruption of wax-rich crystalline phases. DMA indicated that carnauba acts as a reinforcing component, shifting relaxation processes to higher temperatures, whereas jojoba enhances molecular mobility and lowers the α-transition. Beeswax produced intermediate behavior with broadened relaxation profiles. Wettability tests showed that even low additions of beeswax or carnauba markedly increased surface hydrophobicity, whereas jojoba wax resulted in more moderate changes. SEM analysis confirmed a clear morphology–property relationship, showing that moderate wax contents produced a dense and homogeneous TPS structure, while high loadings led to wax-rich phase separation. The study demonstrates that natural waxes serve as effective modifiers of TPS properties, enabling customizable biocomposites suitable for biodegradable and eco-friendly packaging.

Keywords: thermoplastic starch, beeswax, carnauba wax, jojoba wax, biocomposites, biodegradable composites, compression molding.

INTRODUCTION

Currently, due to environmental protection, and obligatory legislation, plastics produced from crude oil are more and more often being replaced by polymers produced from renewable raw materials. Many researchers are focusing on creating biodegradable materials using starch due to its abundance, low cost, non-toxicity, and renewability. However, the inherent water-sensitivity of starch impaired the biocomposites mechanical strength and water vapor barrier properties, the application of starch materials in packaging is greatly limited [1,2]. As a result, starch modification became necessary. Various approaches have been explored to address the hydrophilic characteristics of starch materials, with the addition of hydrophobic agents like oils, fatty acids, waxes, or other plant modifiers proving to be an effective solution [3,4].

Starch is resistant to being processed as a thermoplastic material due to strong intermolecular forces and hydrogen bonds. Therefore, the addition of plasticizers such as glycerin, glycerol, urea, citric acid, glucose, sorbitol, and others is required to produce thermoplastic starch (TPS) [5,6]. The addition of plasticizers increases the flexibility and enhances the processability of

TPS. However, the common use of plasticizers often leads to a higher environmental load; hence, plasticizers should ideally be natural, inexpensive, and renewable to ensure that the production process is both cost-effective and biodegradable.

In many food and non-food applications, starch is modified by chemical methods (acetylation/esterification, acid hydrolysis, cross-linking, grafting, or oxidation) [7,8]. However, the consequent waste generation and high costs demand new alternatives. The waxes are an alternative to current modification methods and changes in starch properties.

Natural waxes such as beeswax (produced by bees), jojoba (obtained from seeds of the plant *Simmondsia chinensis*), and carnauba (obtained from Carnauba palm leaves) have found numerous commercial applications across various industries [9,10]. They are widely used in cosmetics as an ingredient in creams, balms, lipsticks, and hair care products due to their moisturizing, protective, and stabilizing properties. In the food industry, beeswax serves as a protective coating for fruits, extending their shelf life [11]. Additionally, it is employed in pharmaceutical products for wound healing creams and ointments, as well as in candle making for its stability and pleasant aroma. Research has demonstrated that beeswax ranks among the most effective hydrophobic agents for reducing the water sensitivity of starch-based materials [12,13].

Despite their commercial relevance, studies focusing on the effects of these natural waxes on the physicochemical properties of starch-based packaging, particularly fabricated by compression molding, remain limited. Understanding how different wax types and their concentrations influence thermal, mechanical, and surface properties of starch composites is essential to optimize material performance for packaging applications.

This work aims to systematically investigate the incorporation of natural waxes (beeswax, jojoba, and carnauba) into starch matrices prepared by compression molding and to elucidate their impact on the physicochemical characteristics relevant to packaging functionality.

MATERIALS AND METHODS

Materials

Potato starch was produced from Potato Industry Company (Trzemeszno, Poland). Glycerine (M_W = 92.10 g/mol, pure 99.95%) was purchased from PolAura (Morąg, Poland), natural beeswax (T_m = 67.9 °C, ρ = 0.96 g/cm³) was purchased from Szkaradek (Nowy Sącz, Poland), jojoba wax (T_m = 68–70 °C, ρ = 0.86–0.90 g/cm³) (Armadillo, Polska), and carnauba wax (T_m = 80–86 °C, ρ = 0.990–0.999 g/cm³ (Machnijkrem, Polska).

Preparation of samples

Waxes and glycerin were placed in glass beakers (each wax separately) and then heated on a hot plate with a magnetic stirrer (DLAB MS-H280-Pro, Germany) to a temperature of 90 °C until the wax dissolved and evently mixed with the glycerin. Next, native starch, previously dried at 45 °C for 24 hours, was added and stirred until a homogeneous consistency was obtained. Then, the prepared material was compressed using a vulcanization press (AW03, Argenta, Poland) at a pressure of 0.72 MPa for 30 seconds each. Samples containing 1%, 5%, 10%, and 15% beeswax were pressed at a temperature of 160 °C. Meanwhile, samples with 20%, 25%, 30%, and 50% wax content were pressed at 140 °C. To obtain samples of the same thickness after pressing, the prepared material (15 g each time) was placed in a special metal ring with a diameter of 8.5 cm and a thickness of 2 mm (see Figure 1). After pressing, the samples were left to cool and then removed from the mold.

The samples are named as follows: T – starch samples with glycerin (thermoplastic starch), XY – starch samples with glycerin and wax, where X represents the type of wax (B – beeswax, J – jojoba wax, C – carnauba wax), and Y represents the wax content, ranging from 1 to 50%.

Due to the functional range and physicochemical characteristics of the waxes, different concentrations were used. For beeswax, concentrations were 1, 5, 10, 15, 20, 25, 30, and 50%. For jojoba and carnauba waxes, only 5% and 20% were used.

The selection of wax concentrations for the samples was based on several factors. For beeswax, a wide range of concentrations was chosen to enable a comprehensive assessment of its impact on the properties of thermoplastic starch (TPS). For jojoba and carnauba waxes, due to their distinct physicochemical properties and limited solubility in the TPS matrix, two representative concentrations (5% and 20%) were

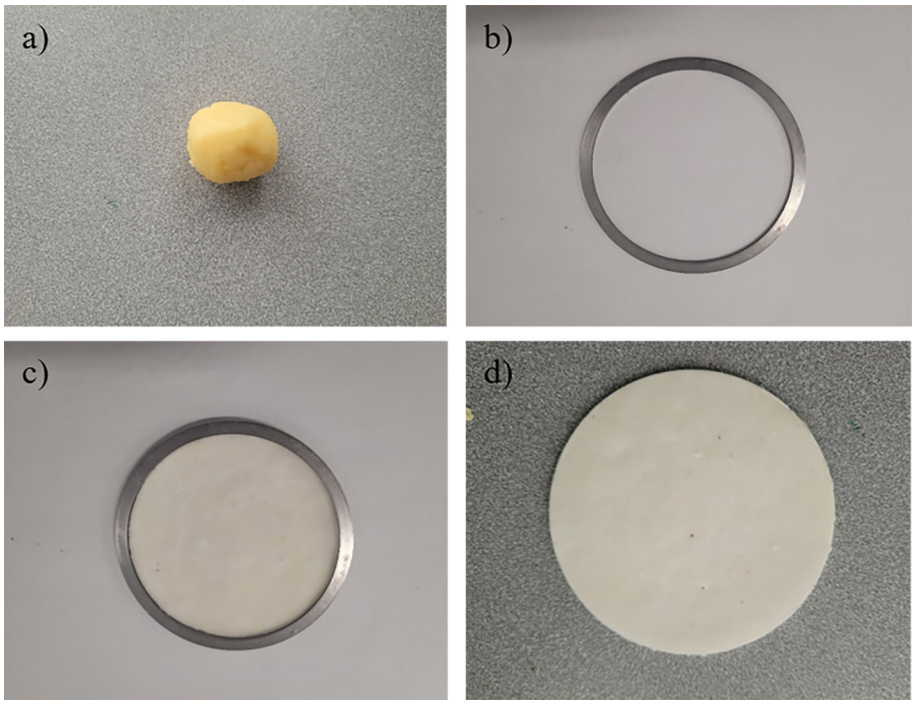

Figure 1. Sample preparation includes: a) the prepared ball, b) a special metal ring, c) the compressed material, and d) the samples removed from the mold

selected. These concentrations were identified in the literature and preliminary studies as sufficient to capture the key effects on material properties [14,15]. Additionally, practical considerations related to mixture stability and sample preparation efficiency influenced the narrower concentration range for these waxes. This approach enables an optimized experimental plan that strikes a balance between representativeness and resource efficiency, facilitating a comparative analysis of the results.

Metodology

Contact angle measurements were performed using the dynamic liquid flow method with a DSA 100 goniometer (Krűss GmbH, Germany) according to the PN-93/C-89438 standard. In this method, a polar liquid (water) and a non-polar liquid (diiodomethane) were used. Drops of the test liquid were applied to the sample, and the instrument measured the dynamic contact angle of the analysed material. For each sample, six contact angle measurements were conducted with water or diiodomethane.

The thermal degradation rate was determined using a Q500 thermogravimetric (TG) analyzer (TA Instruments, USA). The analysis was conducted in a temperature range from 25 °C to 1000 °C with a heating rate of 10 °C per minute under a nitrogen atmosphere. The tested sample weights ranged between 19 and 20 mg.

Phase transition temperatures of the tested samples were determined using a differential scanning calorimeter DSC Q200 (TA Instruments, USA). Measurements were carried out over a temperature range from -80 °C to 200 °C with a heating rate of 10 °C/min under a nitrogen atmosphere. The analysis consisted of three stages: first heating, cooling, and second heating. Only the data from the second heating cycle, which removed the sample's thermal history, were considered for evaluation. Sample masses ranged between 7.2 and 8.5 mg.

Thermomechanical tests were performed using a DMA Q800 dynamic mechanical analyzer (TA Instruments, New Castle, DE, USA). The samples were cuboids with dimensions of 60 × 10 × 4 mm cut from compression-molded test samples. The samples were examined in a dual cantilever mode, at a constant frequency of 1 Hz and controlled amplitude of 15 μm, as a function of temperature ranging from 25 °C to 160 °C.

Surface analysis of the samples was conducted using a Phenom XL scanning electron microscope (ThermoFisher Scientific, Eindhoven, The Netherlands). Before examination, the samples were coated with a thin layer of gold.

RESULT AND DISCUSSION

Wettability

The contact-angle measurements showed a strong influence of natural waxes on the surface polarity of thermoplastic starch. Neat TPS exhibited a low contact angle (31.45°), confirming its highly hydrophilic character. Beeswax markedly increased hydrophobicity even at low concentrations: 1% raised the contact angle to 79.85°, while 5–10% produced values above 100°, indicating the formation of a stable hydrophobic surface layer. A substantial further increase occurred only at 50% beeswax (135.06°), consistent with surface saturation and the accumulation of wax-rich domains. This effect results from the migration of nonpolar long-chain esters toward the surface during processing, forming a continuous hydrophobic coating (Figure 2).

Carnauba wax produced similarly high contact angles (≈101° for 5–20%), though the weaker dependence on concentration reflects its high crystallinity and limited mobility, which restrict its ability to reorganize at the surface.

In contrast, the jojoba wax composites exhibited significantly lower contact angles (47° for J5 and 67.32° for J20). Although these values increased with concentration, the surfaces remained partially hydrophilic. This is attributed to the molecular structure of jojoba wax, which, despite being solid at room temperature, has low crystallinity and forms a soft, weakly ordered phase. As a result, it shows limited segregation to the surface and does not create a continuous hydrophobic film, remaining more uniformly dispersed within the TPS matrix (Figure 3).

TG analysis

The thermal behavior of the starch-based biocomposites containing various amounts of beeswax was investigated by thermogravimetric analysis (TGA), and the corresponding results are presented in Table 1.

The TGA results show that all samples exhibit a multistage degradation pattern typical of starch-based materials. The initial mass loss below ~150 °C corresponds to the evaporation of moisture and volatiles. The main degradation step occurs between 230–350 °C and is associated with the decomposition of starch chains and glycerol [16,17]. The main decomposition temperature (T_d = 285–292 °C) and maximum degradation rate ($T_{d/dT}$ = 309–312 °C) remain nearly unchanged with beeswax addition, indicating that the primary degradation mechanism of TPS is preserved [18,19].

Beeswax mainly influences the onset of degradation. The temperature at 5% mass loss (T_5) increases from 157.48 °C for neat TPS to 214.13 °C at 50% beeswax, reflecting improved initial

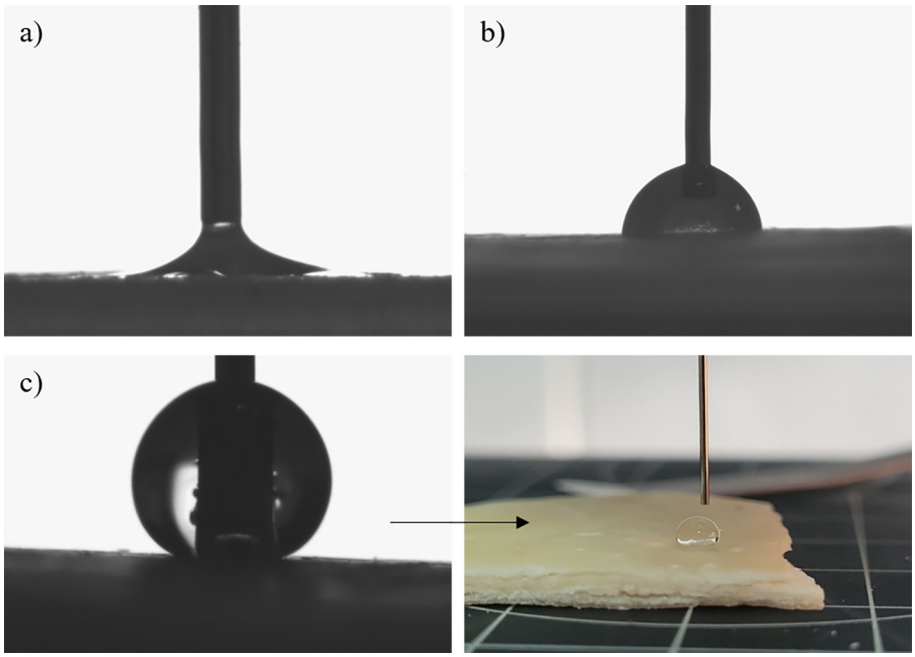

Figure 2. Images of water drops taken during wettability measurements: a) T, b) B5, and c) B50

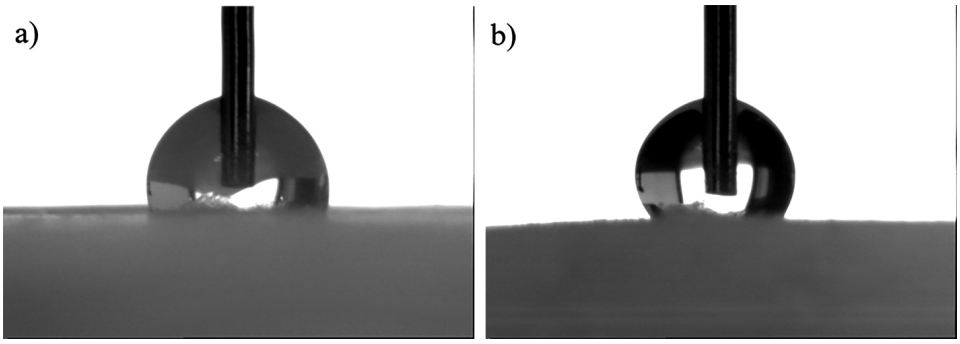

Figure 3. Drop of water on the surface of: a) J20 and b) C20

Table 1. Thermal properties by TGA of biocomposites

Sample	T_d (°C)	$T_{d/dt}$ (°C)	$T_{5\%}$ (°C)	$T_{50\%}$ (°C)	Residue at 980°C (%)
T	290.60	311.67	157.48	306.01	4.45
B1	291.65	311.17	170.02	307.97	8.34
B5	288.25	309.46	159.25	306.55	-
B10	291.40	309.65	177.97	307.58	5.06
B15	290.01	310.66	196.12	308.75	7.60
B20	290.78	308.24	182.36	308.44	3.02
B30	285.88	309.46	173.80	308.89	4.38
B50	285.35	306.42	214.13	313.83	4.23

thermal stability due to the hydrophobic and barrier-forming nature of the wax [14,20]. In contrast, the temperature at 50% mass loss (T_{50}) remains relatively constant (306–314 °C), confirming that the main polysaccharide degradation step is not significantly affected. Residual mass ranged from 3.02% to 8.34%, with differences likely arising from carbonaceous char formation or inorganic fractions present in the wax [18,21].

Figure 4 and Table 2 compare the thermal behavior of composites containing 5% and 20% beeswax, carnauba, and jojoba wax. These concentrations were selected to capture the main effects of each wax type on TPS stability. The analysis shows that all waxes slightly enhance the onset of thermal stability while leaving the principal degradation pathway of TPS unchanged. The main degradation stage occurred between 250 and 350 °C for all samples, corresponding to the thermal decomposition of starch and associated organic components. A minor weight loss below 150 °C was attributed to the evaporation of physically adsorbed moisture and residual glycerol.

The degradation onset temperature (T_d) and the maximum degradation rate temperature ($T_{d/dt}$) are summarized in Table 2. Incorporation of jojoba and carnauba waxes slightly shifted the degradation onset toward higher temperatures (296–298 °C), suggesting improved thermal resistance compared to the neat TPS (T_d = 290.6 °C). In contrast, beeswax-modified samples exhibited slightly lower T_d values, indicating a minor plasticizing effect that could promote earlier chain mobility and decomposition onset. The highest $T_{d/dt}$ was observed for J5 and J20 (313.2 °C and 312.3 °C, respectively), confirming that jojoba wax enhanced the stability of the TPS matrix under heating.

The temperature corresponding to 5% mass loss ($T_{5\%}$) showed a clear stabilizing effect of all waxes, particularly at higher concentrations. The most significant improvement was observed for C20 (T5% = 219.1 °C), reflecting the high melting point and hydrophobic character of carnauba wax, which likely reduces heat and mass transport during early decomposition. Jojoba wax also increased both $T_{5\%}$ and $T_{50\%}$, indicating a more thermally robust dispersion within the TPS matrix. Beeswax provided moderate improvement, especially at 20 wt%, suggesting partial shielding of starch chains without major structural reinforcement.

Residue after heating to 980 °C varied with wax type. Neat TPS left 4.45% residue, while

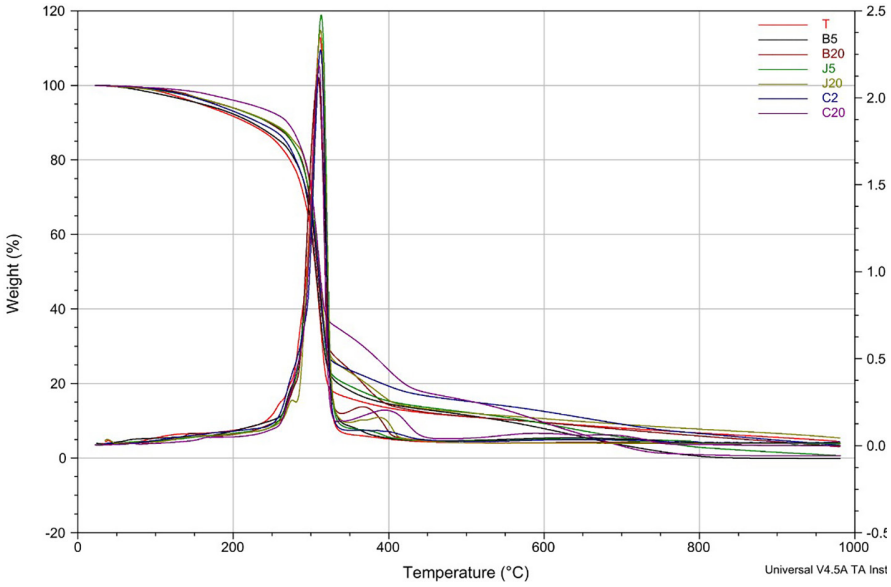

Figure 4. The TG curve and DTG curve of biocomposites

Table 2. Thermal properties by TGA of biocomposites

Sample	T_d (°C)	$T_{d/dt}$ (°C)	$T_{5\%}$ (°C)	$T_{50\%}$ (°C)	Residue at 980°C (%)
T	290.60	311.67	157.48	306.01	4.45
B5	288.25	309.46	159.25	306.55	-
B20	290.78	308.24	182.36	308.44	3.02
J5	296,14	313.21	183.88	310.20	0.65
J20	297,54	312,33	183,76	311,22	5.04
C5	296,66	312,3	175,35	309,78	3.04
C20	294,95	310,26	219,07	311,72	0.58

J20 exhibited the highest value (5.04%), indicating the formation of more stable carbonaceous structures. Conversely, carnauba-containing samples, particularly C20, showed minimal residue (0.58%), consistent with nearly complete volatilization of its aliphatic fraction.

Overall, the results clearly demonstrate that both wax type and concentration significantly influence the thermal degradation profile of samples. Beeswax primarily exhibits plasticizing behavior, slightly reducing degradation onset. Jojoba wax provides the most balanced enhancement, increasing both onset and mid-stage stability and producing the highest char residue. Carnauba wax most strongly delays early degradation, as reflected by its high T5% values, particularly at 20 wt%.

The improved stability observed for higher wax contents (20 wt%) can be attributed to several mechanisms, including hydrophobic barrier effects, wax crystallinity, restricted diffusion of volatiles, interfacial interactions, and the formation of thermally stable residues, as also noted for lipidic additives in starch systems [22,23].

DSC analysis

Differential scanning calorimetry (DSC) cooling thermograms of TPS containing 1–50 wt% beeswax (Figures 5–6) show that wax addition markedly affects the recrystallization behavior of the material. The cooling curves exhibit two exothermic peaks for wax-containing samples, corresponding to the solidification of the low- and high-melting fractions of beeswax, which is a complex mixture of long-chain esters, acids, and hydrocarbons [24,25]. The intensity of these peaks increases with wax concentration, indicating progressive development of crystalline structures.

For neat TPS, a single exothermic peak appears at ~55 °C, associated with retrogradation through amylose/amylopectin double-helix reformation [15]. At low beeswax levels (1–10 wt%), this peak shifts slightly to lower temperatures

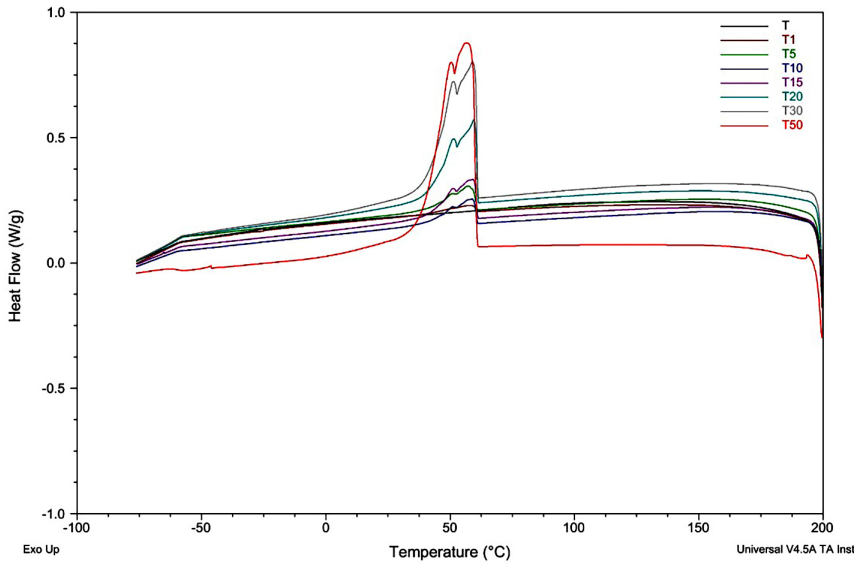

Figure 5. The temperature dependence on the heat flow (DSC solid curve – cooling cycle) of biocomposites

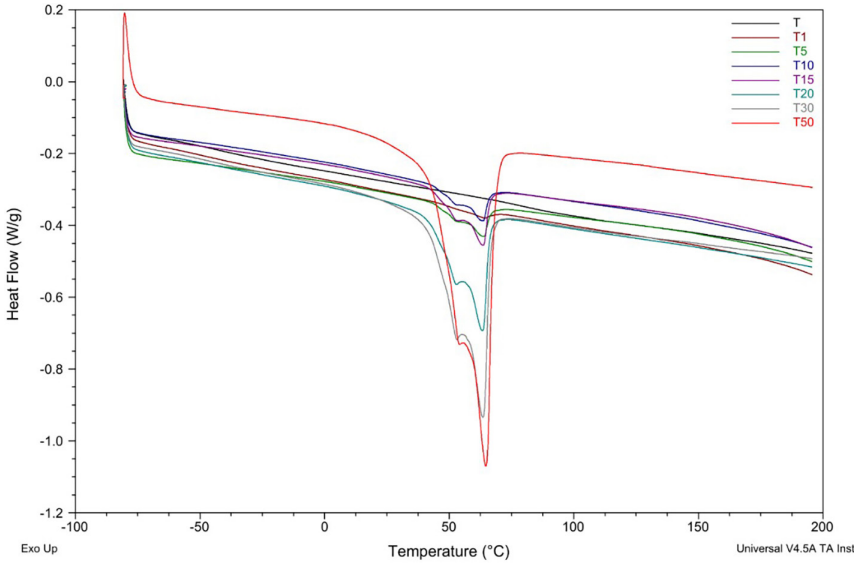

Figure 6. The temperature dependence on the heat flow (DSC solid curve – second heating cycle)

(50–53 °C) and becomes broader, suggesting that beeswax disrupts starch chain mobility and partially inhibits crystallite reformation.

At intermediate wax contents (15–30 wt%), the exothermic event intensifies and shifts upward (55–60 °C), indicating enhanced structural ordering. This behavior is consistent with co-crystallization, where long-chain esters act as nucleating agents that facilitate starch alignment [26]. Such cooperative crystallization has been reported in other starch–lipid systems and can reduce retrogradation rates [15,26].

At 50 wt% beeswax, the thermogram shows a broad, multi-step exothermic transition extending ~45–65 °C. This reflects heterogeneous solidification of wax-rich domains, consistent with phase separation observed in the heating cycle [27]. The wide crystallization range corresponds to the intrinsic complexity of beeswax crystallization, derived from its mixed ester and hydrocarbon composition [24,26].

Overall, DSC cooling results confirm that beeswax strongly modifies TPS recrystallization: low contents hinder starch retrogradation, moderate levels promote more ordered structures via co-crystallization, and very high content leads to phase-separated, multi-domain solidification. These effects highlight the dual role of beeswax as both a structural modifier and crystalline filler in TPS matrices [15,26].

Figure 6 shows the curves correspond to the second heating cycle, allowing for the assessment of the thermal transitions and structural rearrangements occurring after processing and cooling.

In the temperature range from –100 °C to 0 °C, no distinct thermal transitions were detected, indicating that the T_g of the amorphous starch phase is either extremely broad or masked by relaxation processes of the glycerol-plasticized matrix. Such suppression of T_g is common in highly plasticized TPS, where strong hydrogen bonding and high chain mobility blur the glass-transition signal [3,15].

The main endothermic transition for all samples appears between 40 °C and 70 °C and corresponds to the melting of crystalline domains. Neat TPS exhibits a sharp peak at ~52 °C, attributed to the melting of retrograded amylose/amylopectin crystallites [28]. Introducing beeswax causes systematic changes in this region.

At low beeswax contents (1–10 wt%), the melting peak shifts slightly upward (55–58 °C) and broadens, indicating partial miscibility between beeswax and TPS. In this range, beeswax restricts starch chain mobility and promotes more ordered packing, behaving as a structural modifier rather than a plasticizer.

With intermediate beeswax concentrations (15–30 wt%), the melting peak intensifies and shifts to ~58–62 °C. This suggests the formation of co-crystalline regions and increased crystallinity, likely driven by interactions between amylose and long-chain esters in beeswax [26]. The coexistence of starch- and wax-derived crystalline phases improves structural ordering and thermal stability.

At 50 wt% beeswax, the endothermic transition becomes broad and flattened, extending up to ~65 °C. This indicates clear phase separation and the presence of wax-rich domains whose melting behavior overlaps with that of starch. The wide melting interval aligns with the complex thermal profile of natural beeswax, which contains numerous aliphatic esters and hydrocarbons that melt over a broad temperature range [18].

Overall, the DSC heating results show that beeswax strongly impacts the melting behavior of TPS: low contents slightly increase Tm and limit chain mobility, intermediate contents enhance crystallinity through partial co-crystallization, and high contents (≥50 wt%) lead to phase-separated, heterogeneous melting.

Figures 7–8 provide insights into the phase transitions and thermal behavior of TPS modified with 5% and 20% amounts of beeswax, carnauba, and jojoba wax.

Carnauba wax exhibited the highest melting temperatures (≈82 °C) and a marked increase of ΔH_m with wax content (11.66 → 23.19 J/g), indicating the formation of stable, highly crystalline domains. This behavior reflects carnauba's rigid lattice and its ability to nucleate and reinforce crystalline regions within the TPS matrix, resulting in enhanced thermal rigidity and improved ordering upon cooling.

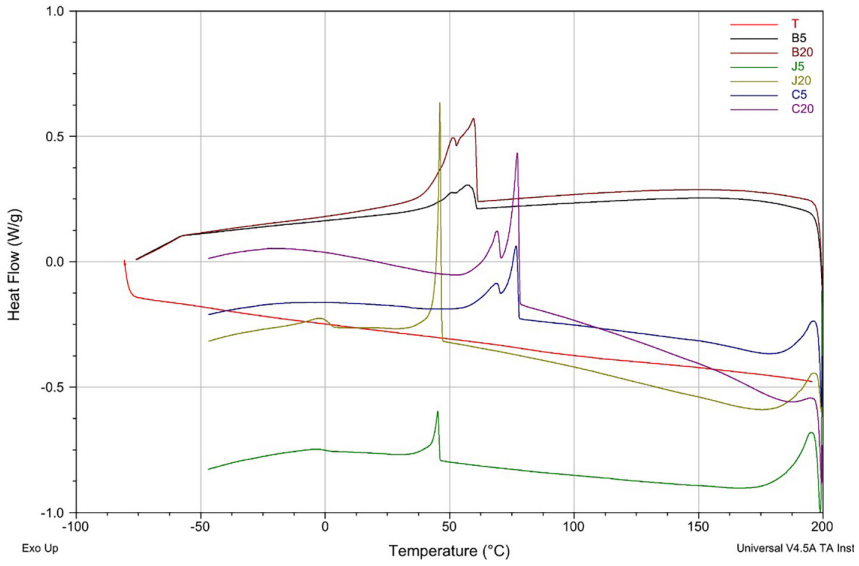

Figure 7. The temperature dependence on the heat flow (DSC solid curve – cooling cycle) of biocomposites

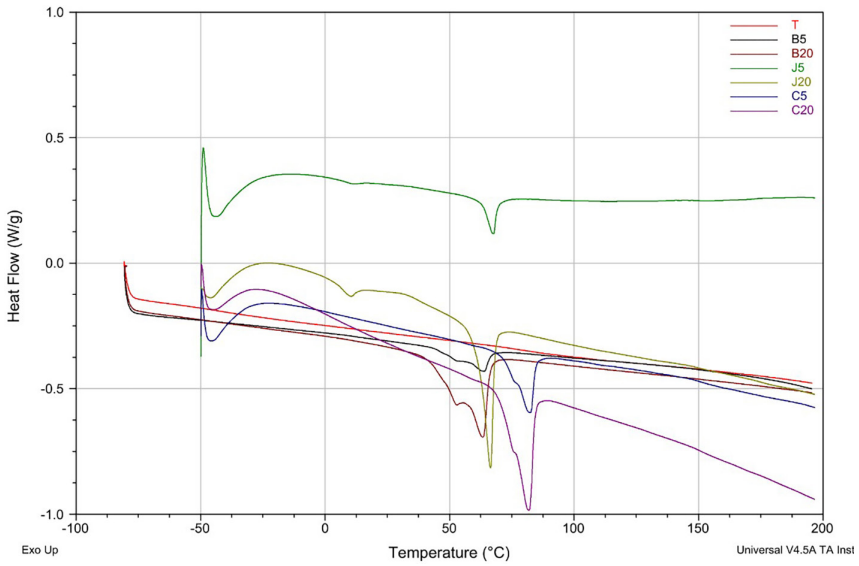

Figure 8. The temperature dependence on the heat flow (DSC solid curve – second heating cycle)

Jojoba-containing samples (J5, J20) showed melting transitions at ≈66–68 °C. Increasing the content from 5 to 20 wt% resulted in a notable rise in ΔH_m (4.11 → 17.89 J/g), demonstrating that higher jojoba concentrations promote the formation of larger or more ordered crystalline regions. Since jojoba wax is solid at room temperature (T_m ≈ 68–70 °C), it provides crystalline – not liquid – domains. The increase in melting enthalpy suggests improved molecular ordering during cooling, possibly through jojoba crystallites alone or joint starch–jojoba co-ordered regions. Although its Tm is lower than that of carnauba, the substantial ΔH_m increase indicates effective structural reinforcement and corresponds with the improved char formation observed in TGA for higher jojoba contents.

Beeswax-containing samples (B5, B20) exhibited melting peaks around 63.2–63.6 °C. At low concentration (B5), ΔHm was relatively small (6.32 J/g), whereas at 20 wt% (B20) ΔHm increased sharply to 26.36 J/g – the highest value among all 20% samples. The nearly unchanged Tm between B5 and B20 indicates that the beeswax crystallites have comparable thermal characteristics at both loadings, but the crystalline fraction grows substantially at 20 wt%. This reveals a concentration-dependent behavior: beeswax acts partially as a softening or plasticizing phase at low amounts, increasing chain mobility, but at higher content transitions into a strongly crystalline filler that contributes significantly to the total crystallinity. This dual mechanism explains why beeswax may exhibit weaker thermal stabilization at low concentrations in TGA, yet strongly increases melting enthalpy at higher loadings.

To summarize comparatively, carnauba acts as a high-T_m, rigid crystalline stabilizer; jojoba forms intermediate-T_m ordered domains that promote recrystallization and homogeneity; and beeswax exhibits concentration-dependent behavior, balancing plasticization and crystallinity. The increase in ΔH_m for all systems correlates with improved phase organization and the formation of hydrophobic, crystalline microstructures that contribute to the improved thermal stability observed in TGA.

The mechanisms of thermal stabilization vary depending on the wax type. Carnauba wax, due to its high crystallinity and high melting temperature, acts as a rigid crystalline barrier that delays thermal decomposition and restricts chain motion. Jojoba wax, with its moderate melting point and semi-crystalline structure, facilitates molecular rearrangement and enhances recrystallization upon heating and cooling, improving homogeneity and char yield. Beeswax exhibits a dual effect: at low concentrations it acts as a plasticizer increasing chain mobility, whereas at high concentrations it behaves as a crystalline filler contributing to enthalpy growth and long-range ordering. Overall, these mechanisms indicate that wax additives not only modify the thermal behavior of TPS but also restructure its microphase organization, reinforcing

stability through hydrophobic interactions and crystalline reinforcement.

DMA analysis

The results of the DMA analysis are presented in Figure 9. The changes in the storage module (E′) and the damping factor (tan δ) as a function of temperature revealed distinct effects depending on wax type and concentration, complementing the dependences observed in TGA and DSC.

The neat sample (T) showed a typical profile of TPS plasticized with glycerol, with E′ = 560 MPa at room temperature, followed by a sharp decrease between 70–90 °C, corresponding to the glass transition temperature (T_g) to rubbery state. The broad tan δ peak in this region reflected the relaxation of starch molecular chains and the onset of viscous flow. This is characteristic of glycerol-plasticized starch systems.

Beeswax-containing materials showed a strongly concentration-dependent response. At low loading (B5), stiffness decreased and a wide tan δ peak was observed, consistent with partial plasticization and limited crystallinity. At 20 wt% (B20), both higher E′ and a narrower, temperature-shifted tan δ peak indicated the formation of a continuous crystalline phase, in line with the high melting enthalpy and thermal stability observed for this formulation.

Jojoba-modified samples also showed a two-stage behavior. J5 exhibited a noticeable modulus drop near the relaxation region, suggesting that dispersed crystalline domains provided only localized reinforcement. At higher content (J20), a lower low-temperature E′ and a tan δ peak shifted to lower temperatures reflected increased molecular mobility due to the formation of semi-continuous wax regions. These features correspond with the increased melting enthalpy and enhanced thermal stability of J20.

Carnauba-containing TPS (C5, C20) showed the strongest reinforcement, maintaining high E′ values over the entire temperature range and displaying sharp, narrow tan δ peaks. This behavior matches its high melting temperature and significant crystallinity, confirming carnauba as an efficient, rigid, thermally stable reinforcing phase.

Processing also influenced the viscoelastic behavior. Compression molding used in this study produces lower molecular orientation and slower cooling compared to injection molding, resulting in slightly lower stiffness but enhanced thermal relaxation and partial recrystallization. Waxes further modulated this morphology through their lubricating and crystallinity-controlling effects, improving interfacial interactions and thermal resistance.

Overall, the waxes tuned the viscoelastic response of TPS through the interplay of plasticization and crystalline reinforcement. Beeswax transitioned from a softening additive at low loading to a reinforcing phase at higher concentrations, jojoba enhanced flexibility and stress dissipation, while carnauba provided the highest stiffness and thermal stability among all formulations.

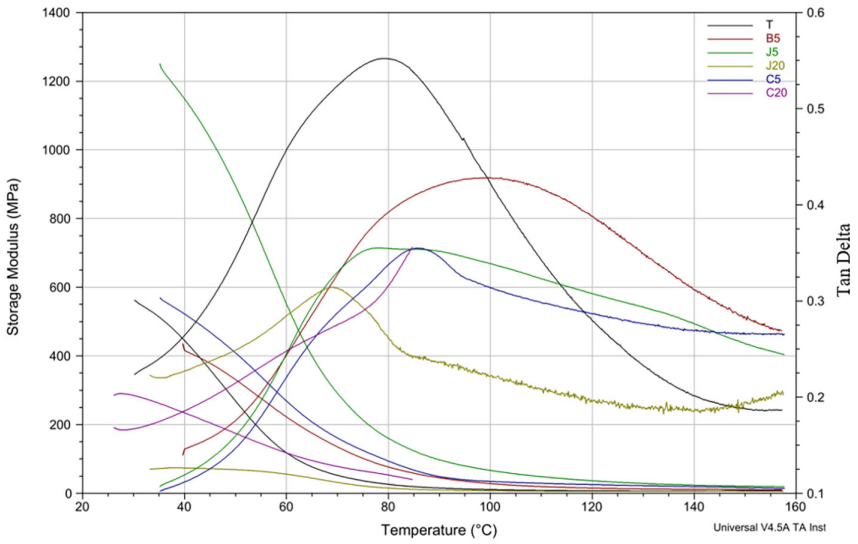

Figure 9. Storage module and Damping coefficient (tanδ) of tested samples as a function of temperature

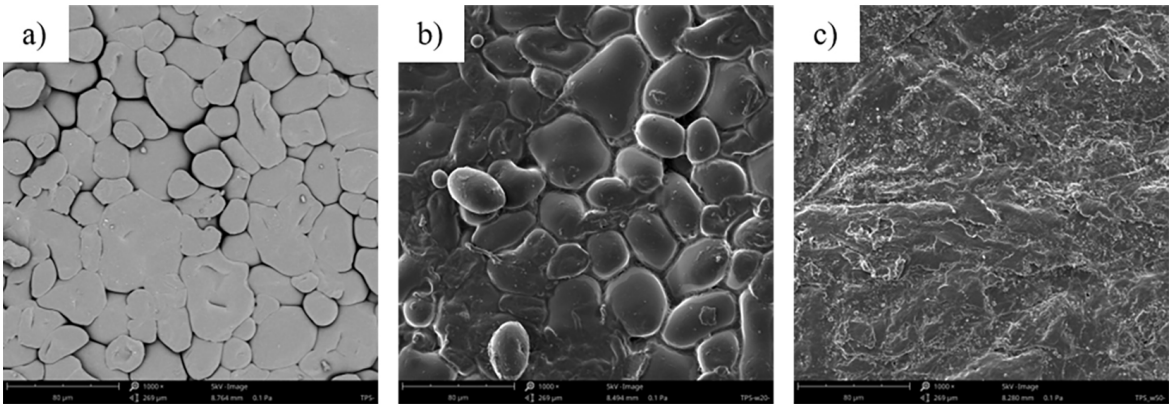

Figure 10. SEM images: a) T, b) B20, c) B50

SEM analysis

The SEM micrographs of the thermoplastic starch and beeswax-modified TPS samples (Figure 10) reveal distinct morphological changes associated with increasing wax content. The unmodified TPS sample (Figure 12a) exhibits a rough and granular surface with partially fused starch granules and visible intergranular voids. This morphology reflects incomplete melting and consolidation of starch domains during compression molding, a common feature in thermoplastic starch systems.

The introduction of a small amount of beeswax to 5% resulted in a smoothing of the surface and partial embedding of starch granules within a continuous matrix. The wax likely acts as a compatibilizing and lubricating phase, filling voids and promoting improved cohesion between starch domains. At this stage, the microstructure still retained some granular features, indicating partial phase separation.

With higher beeswax contents to 20%, the morphology evolved towards a more homogeneous and compact structure. The starch granules appeared increasingly fused, and the continuous phase became dominant. The B20 sample exhibits a smooth, dense surface with minimal porosity, suggesting optimal dispersion and interaction between the starch and wax phases. This microstructure correlates well with the enhanced thermal stability and higher crystallinity observed in the TGA and DSC analyses, as well as the increased storage modulus noted in DMA measurements.

At even higher wax loadings from 25% to 50%, the structure changed again, showing the appearance of microphase separation and the formation of wax-rich domains. The surface was becoming more heterogeneous, and distinct globular or lamellar regions appeared, likely corresponding to recrystallized beeswax aggregates.

CONCLUSION

The study demonstrated that the incorporation of natural waxes significantly influences the structure and properties of thermoplastic starch. The thermal analyses showed that carnauba, beeswax, and jojoba modify the melting behavior and thermal stability of TPS in distinct ways, with clear concentration-dependent effects. Dynamic mechanical analysis revealed systematic changes in viscoelastic behavior, including shifts in relaxation temperatures and variations in storage modulus associated with each type of wax. Surface wettability measurements confirmed that the addition of waxes increases hydrophobicity to differing extents depending on the additive. SEM observations showed that increasing wax content leads to a transition from partially granular structures to homogeneous matrices, followed by microphase separation at the highest loadings. Altogether, the results provide a comprehensive characterization of the relationships between wax type, concentration, and the resulting thermal, mechanical, and morphological features of wax-modified TPS biocomposites.

Acknowledgments

This work was supported by the Ministry of Science and Higher Education [grant numbers MNiSW/2020/347/DIR].

REFERENCES

1. Jabeen, N.; Majid, I.; Nayik, G.A. Bioplastics and food packaging: A review. Cogent Food Agric. 2015:1, https://doi.org/10.1080/23311932.2015.1117749
2. Khan, B.; Bilal Khan Niazi, M.; Samin, G.; Jahan, Z. Thermoplastic starch: A possible biodegradable food packaging material—A review. J. Food Process Eng. 2017;40, https://doi.org/10.1111/jfpe.12447
3. Stepczyńska, M.; Rytlewski, P.; Moraczewski, K.; Pawłowska, A.; Karasiewicz, T. Novel biocomposite of starch and flax fiber modified with tannic acid with biocidal properties. Polymers (Basel). 2024:16, https://doi.org/10.3390/polym16081108
4. Liu, R.; Zhang, R.; Zhai, X.; Li, C.; Hou, H.; Wang, W. Effects of beeswax emulsified by octenyl succinate starch on the structure and physicochemical properties of acid-modified starchfilms. Int. J. Biol. Macromol. 2022;219:262–272, https://doi.org/10.1016/J.IJBIOMAC.2022.07.235
5. Gamarano, D. de S.; Pereira, I.M.; da Silva, M.C.; Mottin, A.C.; Ayres, E. Crystal Structure Transformations in Extruded Starch Plasticized with Glycerol and Urea. Polym. Bull. 2020;77:4971–4992, https://doi.org/10.1007/S00289-019-02999-2/FIGURES/15
6. Jia, P.; Xia, H.; Tang, K.; Zhou, Y. Plasticizers derived from biomass resources: A short review. Polym. 2018;10:1303, https://doi.org/10.3390/POLYM10121303
7. Oktay, S.; Pizzi, A.; Köken, N.; Bengü, B. Chemical modification techniques of corn starch for synthesis wood adhesive. Int. J. Adhes. Adhes. 2024;128:103545, https://doi.org/10.1016/J.IJADHADH.2023.103545
8. Sudheesh, C.; Pillai, S. A review on research advances in efficient approaches to augment hydrothermal techniques for starch functionalization: Mechanisms, Properties and Potential Food Applications. Carbohydr. Polym. 2025;357:123441, https://doi.org/10.1016/J.CARBPOL.2025.123441.
9. Agarwal, S.; Arya, D.; Khan, S. Comparative fatty acid and trace elemental analysis identified the best raw material of jojoba (*Simmondsia Chinensis*) for commercial applications. Ann. Agric. Sci. 2018;63:37–45, https://doi.org/10.1016/J.AOAS.2018.04.003
10. Santos, A. de A. dos; Matos, L.C.; Mendonça, M.C.; Lago, R.C. do; Muguet, M.C. dos S.; Damásio, R.A.P.; Ponzecchi, A.; Soares, J.R.; Sanadi, A.R.; Tonoli, G.H.D. Evaluation of paper coated with cationic starch and carnauba wax mixtures regarding barrier properties. Ind. Crops Prod. 2023;203:117177, https://doi.org/10.1016/J.INDCROP.2023.117177
11. Chiumarelli, M.; Hubinger, M.D. Stability, solubility, mechanical and barrier properties of cassava starch – carnauba wax edible coatings to preserve fresh-cut apples. Food Hydrocoll. 2012;28:59–67, https://doi.org/10.1016/J.FOODHYD.2011.12.006
12. Omar-Aziz, M.; Khodaiyan, F.; Yarmand, M.S.; Mousavi, M.; Gharaghani, M.; Kennedy, J.F.; Hosseini, S.S. Combined effects of octenylsuccination and beeswax on pullulan films: water-resistant and mechanical properties. Carbohydr. Polym. 2021;255:117471, https://doi.org/10.1016/J.CARBPOL.2020.117471
13. Pérez-Vergara, L.D.; Cifuentes, M.T.; Franco, A.P.; Pérez-Cervera, C.E.; Andrade-Pizarro, R.D. Development and characterization of edible films based on native cassava starch, beeswax, and propolis. NFS J. 2020;21:39–49, https://doi.org/10.1016/J.NFS.2020.09.002
14. Hafila, K.Z.; Jumaidin, R.; Ilyas, R.A.; Selamat, M.Z.; Yusof, F.A.M. Effect of palm wax on the mechanical, thermal, and moisture absorption properties of thermoplastic cassava starch composites. Int. J. Biol. Macromol. 2022;194:851–860, https://doi.org/10.1016/J.IJBIOMAC.2021.11.139
15. Diyana, Z.N.; Jumaidin, R.; Selamat, M.Z.; Suan, M.S.M. Thermoplastic starch/beeswax blend: characterization on thermal mechanical and moisture absorption properties. Int. J. Biol. Macromol. 2021;19:224–232, https://doi.org/10.1016/J.IJBIOMAC.2021.08.201
16. Liu, X.; Wang, Y.; Yu, L.; Tong, Z.; Chen, L.; Liu, H.; Li, X. Thermal degradation and stability of starch under different processing conditions. Starch - Stärke 2013;65:48–60, https://doi.org/10.1002/STAR.201200198
17. Zhang, D.; Cao, Y.; Zhang, P.; Liang, J.; Xue, K.; Xia, Y.; Qi, Z. Investigation of the thermal decomposition mechanism of glycerol: The combination of a theoretical study based on the Minnesota functional and experimental support. Phys. Chem. Chem. Phys. 2021;23:20466–20477, https://doi.org/10.1039/D1CP01526E
18. Neznakomova, M.P.; Salaün, F.; Dineff, P.D.; Tsanev, T.D.; Gospodinova, D.N. Structural and thermal effects of beeswax incorporation in electrospun PVA nanofibers. Materials (Basel). 2025;18:3293, https://doi.org/10.3390/MA18143293
19. Zhang, Y.; Simpson, B.K.; Dumont, M.J. Effect of beeswax and carnauba wax addition on properties of Gelatin Films: A comparative study. Food Biosci. 2018;26:88–95, https://doi.org/10.1016/J.FBIO.2018.09.011
20. Gigante, V.; Cinelli, P.; Righetti, M.C.; Sandroni, M.; Polacco, G.; Seggiani, M.; Lazzeri, A. On the use of biobased waxes to tune thermal and mechanical properties of polyhydroxyalkanoates–bran

biocomposites. Polym. 2020;12:2615, https://doi.org/10.3390/POLYM12112615

21. Ren, L.; Cai, Y.; Ren, L.; Yang, H. Preparation of modified beeswax and its influence on the surface properties of compressed poplar wood. Materials (Basel). 2016;9:230, https://doi.org/10.3390/MA9040230
22. Li, Q.; Gao, Y.; Li, Y.; Du, S. kui; Yu, X. Effect of hydrophilic groups in lipids on the characteristics of starch–lipid complexes. Int. J. Food Sci. Technol. 2023;58:4862–4871, https://doi.org/10.1111/IJFS.15835
23. Majeed, T.; Dar, A.H.; Pandey, V.K.; Dash, K.K.; Srivastava, S.; Shams, R.; Jeevarathinam, G.; Singh, P.; Echegaray, N.; Pandiselvam, R. Role of additives in starch-based edible films and coating: a review with current knowledge. Prog. Org. Coatings 2023;181:107597, https://doi.org/10.1016/J.PORGCOAT.2023.107597
24. Moghtadaei, M.; Soltanizadeh, N.; Goli, S.A.H. Production of sesame oil oleogels based on beeswax and application as partial substitutes of animal fat in beef burger. Food Res. Int. 2018;108:368–377, https://doi.org/10.1016/J.FOODRES.2018.03.051
25. Liu, C.; Zheng, Z.; Shi, Y.; Zhang, Y.; Liu, Y. Development of low-oil emulsion gel by solidifying oil droplets: Roles of internal beeswax concentration. Food Chem. 2021;345:128811, https://doi.org/10.1016/J.FOODCHEM.2020.128811
26. Luchesi, B.R.; Kley, F.; Moreira, V.; Marconcini, J.M.; Luis, W.; Paulo, S.; Correspondence, B. Scalable production of hydrophobic starch/beeswax films by continuous solution casting. J. Appl. Polym. Sci. 2024;141:e54730, https://doi.org/10.1002/APP.54730
27. Buchwald, R.; Breed, M.D.; Greenberg, A.R. The thermal properties of beeswaxes: unexpected findings. J. Exp. Biol. 2008;211:121–127, https://doi.org/10.1242/JEB.007583
28. Li, C. Unraveling the complexities of starch retrogradation: insights from kinetics, molecular interactions, and influences of food ingredients. Food Rev. Int. 2024;40:3159–3182, https://doi.org/10.1080/87559129.2024.2347467;wgroup:string:publication